

## Nonmesonic Decays of ${}^{\Lambda}H$ , ${}^{\Lambda}He$ and ${}^{\Lambda}He$ Hypernuclei by the $\pi$ and $\rho$ Exchange Model

Kiyokazu TAKEUCHI, Hideo TAKAKI\* and Hiroharu BANDŌ  
Division of Mathematical Physics, Fukui University, Fukui 910

\*Division of General Education, Fukui Institute of Technology, Fukui 910

(Received November 17, 1984)

The nonmesonic decay rates of  ${}^{\Lambda}H$ ,  ${}^{\Lambda}He$  and  ${}^{\Lambda}He$  are evaluated by employing the  $\pi$  and  $\rho$  exchange model with realistic  $\Lambda N$  and  $NN$  correlation functions. The tensor dominating nature characterizes the decay interaction in this model and gives very different decay rates for  ${}^{\Lambda}H$  and  ${}^{\Lambda}He$ .

The nonmesonic (nm) decay mode  $\Lambda + N \rightarrow N + N + 176$  MeV which takes place only in nuclei, is considered to dominate the pionic decay mode  $\Lambda \rightarrow N + \pi + 40$  MeV with increasing mass number of the hypernucleus, because the Pauli exclusion principle suppresses the latter mode quite strongly. The lifetimes of heavy hypernuclei are thus determined by the nm decay rates.

The properties of the nm decay interaction were investigated by Block and Dalitz<sup>1)</sup> by performing a quite simple analysis of the available data on  ${}^{\Lambda}H$  and  ${}^{\Lambda}He$ . Their conclusion was the " $({}^3S_1)_{\Lambda N} \rightarrow ({}^3P_1)_{NN}$  dominance". There have been attempts to explain such a feature of the nm decay interaction.<sup>2)-7)</sup> On the other hand, to predict the lifetime of heavy hypernuclei, the nm decay rate of a  $\Lambda$  particle in infinite nuclear matter was evaluated by employing the  $\pi$  (and  $\rho$ ) exchange model<sup>8),9)</sup> or the quark hybrid model.<sup>10)</sup>

The aim of this note is to apply the  $\pi$  and  $\rho$  exchange model to estimate the nm decay rates of the  ${}^{\Lambda}H$ ,  ${}^{\Lambda}He$  and  ${}^{\Lambda}He$  hypernuclei for which some experimental data are available. In this model the nm decay interaction is generated by the diagram depicted in Fig. 1 where  $w$  and  $s$  indicate the weak and strong Hamiltonians,  $H_w$  and  $H_s$ , respectively. For the  $\pi$  exchange, we adopt the effective Hamiltonian  $H_w^\pi$  which describes the pionic decay of  $\Lambda$  and the standard  $NN\pi$  coupling as  $H_s^\pi$ ,

$$H_w^\pi = g_w \bar{\psi}_N (1 + \lambda \gamma_5) \tau \Psi_\Lambda \phi_\pi, \quad (1)$$

$$g_w = 0.24 \times 10^{-6}, \quad \lambda = -6.9, \quad (2)$$

$$H_s^\pi = g_s \bar{\psi}_N \gamma_5 \tau \psi_N \phi_\pi, \quad (3)$$

$$g_s^2 / 4\pi = 14, \quad (4)$$

where  $\Psi_\Lambda = \begin{pmatrix} 0 \\ \phi_\Lambda \end{pmatrix}$  is the spurion with  $\phi_\Lambda$  being the  $\Lambda$  field, which is introduced to conveniently take

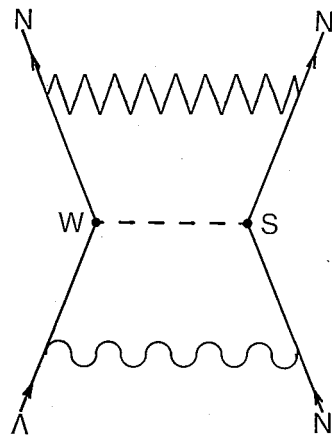


Fig. 1. The meson-exchange diagram which generates the nm decay interaction. The wavy and zigzag lines denote the initial and final state interactions, respectively.

account of the  $\Delta I = 1/2$  rule.

Combining  $H_w^\pi$  and  $H_s^\pi$ , we obtain the nm decay interaction  $V_\pi$ ,

$$\begin{aligned} V_\pi &= -\frac{g_w g_s}{4\pi} \lambda \frac{m_\pi^2}{4MM_N} m_\pi Y(x) \\ &\quad \times \left\{ \frac{1}{3} (\boldsymbol{\sigma}_1 \boldsymbol{\sigma}_2) + T(x) S_{12} \right\} (\boldsymbol{\tau}_1 \boldsymbol{\tau}_2) \\ &\quad + i \frac{g_w g_s}{4\pi} \frac{m_\pi}{2M_N} m_\pi Y(x) V(x) (\boldsymbol{\sigma}_2 \boldsymbol{r}) (\boldsymbol{\tau}_1 \boldsymbol{\tau}_2) \\ &\equiv \{ V_\pi^C(r) (\boldsymbol{\sigma}_1 \boldsymbol{\sigma}_2) + V_\pi^T S_{12} \\ &\quad + V_\pi^V(r) (\boldsymbol{\sigma}_2 \boldsymbol{r}) \} (\boldsymbol{\tau}_1 \boldsymbol{\tau}_2), \end{aligned} \quad (5)$$

$$Y(x) = \frac{e^{-x}}{x}, \quad T(x) = \frac{1}{3} + \frac{1}{x} + \frac{1}{x^2},$$

$$V(x) = 1 + \frac{1}{x}, \quad (6)$$

where  $x \equiv m_\pi r$ ,  $\bar{M} = (M_\Lambda + M_N) / 2$  and the suffix 1 refers to  $\Lambda$ .

The  $\rho$  exchange interaction was discussed in detail by McKellar and Gibson.<sup>9)</sup> Although there are much ambiguities, we use here the  $V_\rho$  obtained by the factorization model,<sup>9)</sup> of which the most important tensor term is expressed as

$$V_\rho^T = \pm \frac{G_F m_\rho^2 (1 + \chi_\rho)(1 + \chi_\lambda)}{4\pi} \frac{m_\rho^2}{4\sqrt{3}} \frac{m_\rho^2}{4\bar{M}M_N} \times m_\rho x Y(x) V(x) S_{12}(\tau_1 \tau_2), \quad (7)$$

$$G_F = 1.166 \times 10^{-5} (\text{GeV})^{-2},$$

$$\chi_\rho = 6.6, \quad \chi_\lambda = 0.6\chi_\rho, \quad x \equiv m_\rho r.$$

The  $\pm$  sign in front accounts for the theoretically uncertain phase relative to  $V_\pi$ .

When the form factors with a standard shape are introduced, the functions appearing in Eqs. (5) and (7) are to be replaced as

$$V_\pi^C; Y(x) \rightarrow Y(x) - \left(\frac{\Lambda_\pi}{m_\pi}\right)^3 Y(x), \quad (8)$$

$$V_\pi^T; Y(x) T(x) \rightarrow Y(x) T(x) - \left(\frac{\Lambda_\pi}{m_\pi}\right)^3 Y(x) T(x), \quad (9)$$

$$V_\pi^V; Y(x) V(x) \rightarrow Y(x) V(x) - \left(\frac{\Lambda_\pi}{m_\pi}\right)^2 Y(x) V(x), \quad (10)$$

where  $X \equiv \Lambda_\pi r$  and

$$V_\rho^T; x Y(x) V(x) \rightarrow x Y(x) V(x) + \left(\frac{\Lambda_\rho}{m_\rho}\right) X Y(X) V(X) - 12 \frac{m_\rho^2}{\Lambda_\rho^2 - m_\rho^2} \left\{ Y(x) T(x) - \left(\frac{\Lambda_\rho}{m_\rho}\right)^3 Y(X) T(X) \right\}, \quad (11)$$

where  $X \equiv \Lambda_\rho r$ . The cutoff masses used in Ref. 9) are  $\Lambda_\pi^2 = 20m_\pi^2$  and  $\Lambda_\rho^2 = 2.27m_\rho^2$ .

The nm decay rate  $\Gamma_{nm}$  of the  ${}^A_Z$  hypernucleus is expressed by

$$\Gamma_{nm} = 4\pi \sum \int \frac{d^3 k}{(2\pi)^3} \int \frac{d^3 K}{(2\pi)^3} \times \delta\left(\frac{\mathbf{k}^2}{M_N} + \frac{\mathbf{K}^2}{4M_N} - M_A + M_N - \epsilon_A - \epsilon_N\right) \times |\langle \Phi(A-2) e^{i\mathbf{k}\mathbf{r}} e^{i\mathbf{K}\mathbf{R}} | \times \sum_N (V_\pi + V_\rho) | \Phi({}^A_Z) \rangle|^2, \quad (12)$$

where  $\sum$  represents the summation over the final state spin direction and the average over the initial state spin direction. The relative and cm momenta (coordinates)  $\mathbf{k}(\mathbf{r})$  and  $\mathbf{K}(\mathbf{R})$  refer to

two nucleons emitted after the nm decay interaction. The residual nucleus,  $\Phi(A-2)$ , is assumed to be in its ground state. The  $(\epsilon_A + \epsilon_N)$  is the binding energy difference between  $\Phi({}^A_Z)$  and  $\Phi(A-2)$ .

We express the hypernuclear wave functions (wf)  $\phi({}^A_Z)$  for  ${}^1\text{H}$ ,  ${}^1\text{He}$  and  ${}^3\text{He}$  as

$$\Phi({}^A_Z) = \Phi({}^{A-1}Z) \phi_A(r_A), \quad (13)$$

where the nuclear wfs  $\Phi({}^{A-1}Z)$  are described by Gaussians with appropriate size parameters ( $b_N = 1.36\text{fm}$  for  ${}^4\text{He}$  and  $1.65\text{fm}$  for  ${}^3\text{H}$  and  ${}^3\text{He}$ ) and  $\phi_A(r_A)$  is the  $s$ -state wf of the  $\Lambda$ -nucleus relative coordinate  $r_A$ . The spin couplings ( $J^\pi = 0^+$  for  ${}^1\text{H}$  and  ${}^1\text{He}$  and  $J^\pi = 1/2^+$  for  ${}^3\text{He}$ ) are implicit. We obtain  $\phi_A(r_A)$  by solving the equation of the folding potential model which is derived from the  $\Lambda N$   $G$ -matrix<sup>11)</sup> for the Nijmegen model  $D$  interaction.<sup>12)</sup> By expanding  $\phi_A(r_A)$  in terms of the harmonic oscillator (h.o.) wfs  $u$  and making a Moshinsky transformation, we rewrite Eq. (13) as

$$\Phi({}^A_Z) = \Phi(A-2) \sum_L \sum_{nN} w_L(nN) u_{nL}(r) u_{NL}(R) \times [Y_L(\hat{\mathbf{r}}) \times Y_L(\hat{\mathbf{R}})]_0. \quad (14)$$

We take only the  $L=0$  part by assuming that the nm decay starts from the  $\Lambda N$   $S$ -states. The weight of the  $S$ -states,  $\sum_{nN} w_0(nN)^2$ , amounts to 0.84 for  ${}^1\text{He}$  and 0.88 for  ${}^1\text{H}({}^1\text{He})$ . The  $w_0(nN)$  is distributed rather widely to higher  $(n, N)$  quanta.

Equation (12) is now reduced to

$$\Gamma_{nm} = 4M_N \sum_{i=p,n} \sum_{T=0,1} \sum_c W(S_i, t) \int_0^{K_x} dK K^2 k \times |\sum_{nN} w_0(nN) (-)^N u_{N0}(K) \times \langle j_L(kr) \mathcal{Y}_{LS_f \mathcal{J}} \xi_T | V_\pi + V_\rho | u_{n0}(r) \mathcal{Y}_{0S_i \mathcal{J}} \xi_i \rangle|^2, \quad (15)$$

$$c \equiv \{S_i LS_f \mathcal{J} = S_i\},$$

where  $k$  is a function of  $K$

$$k = \frac{1}{2} \sqrt{K_x^2 - K^2},$$

$$K_x = 2\sqrt{M_N(M_A - M_N + \epsilon_A + \epsilon_N)}. \quad (16)$$

The function  $W(S_i, t)$  denotes the number of the  $\{\Lambda t (t=p \text{ or } n), \text{ spin } S_i\}$  bond, as given in Table I. The isospin functions for  $NN$  and  $\Lambda N$  are denoted by  $\xi_T$  and  $\xi_i$ , respectively.

The kinematical properties of  $V_\pi$  and  $V_\rho$  allow the six types of transitions,

$$\begin{aligned}
 &({}^1S_0)_{AN} \rightarrow ({}^1S_0)_{NN}, ({}^3P_0)_{NN}, \quad (T=1) \\
 &({}^3S_1)_{AN} \rightarrow ({}^3S_1)_{NN}, ({}^3D_1)_{NN}, ({}^1P_1)_{NN}, \quad (T=0) \\
 &\quad \rightarrow ({}^3P_1)_{NN}. \quad (T=1)
 \end{aligned} \tag{17}$$

Each transition is induced by one of the  $V^C$ ,  $V^T$  and  $V^V$  components.

The initial ( $AN$ ) and final ( $NN$ ) state correlations are introduced, as depicted in Fig. 1, by solving the  $AN$  Bethe-Goldstone equations and the  $NN$  scattering equations, respectively, with the Nijmegen model  $D$  interactions.<sup>12)</sup> We make the replacements in Eq. (15),

$$\begin{aligned}
 u_{n0}(r) \mathcal{Y}_{0S_1S_1} \rightarrow f_{S_1}(r) u_{n0}(r) \mathcal{Y}_{0S_1S_1} \\
 + \delta_{S_11} f_2(r) \mathcal{Y}_{211}, \tag{18} \\
 j_L(kr) \mathcal{Y}_{LS_1g} \rightarrow \Psi_{LS_1g}(k, r) \mathcal{Y}_{LS_1g} \\
 + \delta_{S_11} \{ \delta_{L0} \chi_2(k, r) \mathcal{Y}_{211} \\
 + \delta_{L2} \chi_0(k, r) \mathcal{Y}_{011} \}, \tag{19}
 \end{aligned}$$

where  $f_2$ ,  $\chi_2$  and  $\chi_0$  are induced by the tensor forces and play important roles.

Table II shows the dependences of the six channel-contributions on the form factor (F) and the initial and final state correlations (C). In the {no F, no C} case, the  $({}^3S_1)_{AN} \rightarrow ({}^3D_1)_{NN}$  channel

Table I. The number of  $\{At, \text{spin } S_i\}$  bonds ( $t=p$  or  $n$ ).

$(t, S_i)$	$(p, 0)$	$(n, 0)$	$(p, 1)$	$(n, 1)$
${}^1H$	1	1/2	0	3/2
${}^1He$	1/2	1	3/2	0
${}^3He$	1/2	1/2	3/2	3/2

Table II. Dependences of the channel contributions to  $\Gamma_{nm}({}^1He)$  on the form factor (F) and the initial and final state correlations (C).

	F	C	${}^1S_0 - {}^1S_0$	${}^1S_0 - {}^3P_0$	${}^3S_1 - {}^3S_1$	${}^3S_1 - {}^3D_1$	${}^3S_1 - {}^1P_1$	${}^3S_1 - {}^3P_1$	Sum
$\pi$	N	N	${}^3_{0.040}$	0.011	${}^2_{0.012}$	0.352	0.100	0.022	0.487
	$p$	Y	${}^2_{0.089}$	${}^2_{0.053}$	0.027	0.161	0.048	0.011	0.261
	$n$	Y	${}^3_{0.015}$	${}^2_{0.028}$	0.092	0.038	${}^2_{0.028}$	${}^2_{0.011}$	0.137
	$n$	Y	${}^3_{0.029}$	${}^2_{0.056}$	—	—	—	${}^2_{0.022}$	0.008
$\rho$	N	N	*	*	*	1.319	*	*	1.319
	$p$	Y	*	*	*	0.081	*	*	0.081
	$n$	Y	*	*	0.094	${}^2_{0.036}$	*	*	0.097
	$n$	Y	*	*	—	—	—	*	*

N=No, Y=Yes. (in units of  $\Gamma_\lambda$ )

—: not allowed by the Pauli principle.

\*: no contributions from  $V_\rho^T$ .

decay is by far the strongest, for which the tensor interactions  $V_\pi^T$  and  $V_\rho^T$  are responsible. As F and C are introduced successively, this channel contributions decrease significantly. Instead, the  $({}^3S_1)_{AN} \rightarrow ({}^3S_1)_{NN}$  decay is largely enhanced due to the induced  $({}^3D_1)_{NN}$  wave which allows the action of the strong tensor ( $V_\pi^T$  and  $V_\rho^T$ ) nm decay interactions. Thus the cooperation of the  $NN$  tensor and the nm decay tensor interactions yields the large enhancement.

Table III summarizes the results for  ${}^5He$ ,  ${}^4He$  and  ${}^4H$ , where  $\pi + \rho$  and  $\pi - \rho$  correspond to two possible relative phases. The  $\pi$  and  $\rho$  contributions are comparable in magnitude in the dominant  $({}^3S_1)_{AN} \rightarrow ({}^3S_1)_{NN}$  channel. Therefore, the  $\pi + \rho$  combination leads to an efficient amplification, while  $\pi - \rho$  a complete cancellation. In  ${}^4H$ , the most important channels  $({}^3S_1)_{AN} \rightarrow ({}^3S_1, {}^3D_1)_{NN}^{T=0}$  are missing, because these final  $NN$  states are reached only from the  $\Lambda p$  pair, while the  $\Lambda p$  pair in  ${}^4H$  is in the  ${}^1S_0$  state (see Table I). Thus the resulting  $\Gamma_{nm}$  of  ${}^4H$  is particularly small.

Compared with the "exp" values<sup>9)</sup> given in the last column of Table III, the calculated " $\pi + \rho$ " value of  ${}^5He$  has reasonable magnitude, while those of  ${}^4He$  and  ${}^4H$  are not consistent even qualitatively.

We have estimated the nm decay rates of  ${}^4H$ ,  ${}^4He$  and  ${}^5He$  by employing the  $\pi$  and  $\rho$  exchange model together with the realistic  $AN$  and  $NN$  correlation functions. This model is characterized by the tensor dominating nature,

Table III. Summary of the calculated  $\Gamma_{nm}$  (in units of  $\Gamma_\lambda$ ) for  ${}^5\text{He}$ ,  ${}^4\text{He}$  and  ${}^3\text{H}$ . The cases of two possible relative phases of  $\pi$  and  $\rho$  contributions are shown. The "exp" values are from the analysis of Ref. 1).

		${}^1S_0 \rightarrow {}^1S_0$	${}^1S_0 \rightarrow {}^3P_0$	${}^3S_1 \rightarrow {}^3S_1$	${}^3S_1 \rightarrow {}^3D_1$	${}^3S_1 \rightarrow {}^1P_1$	${}^3S_1 \rightarrow {}^3P_1$	Total	"exp"
${}^5\text{He}$	$\pi$ alone	0.044	0.083	0.092	0.038	0.028	0.032	0.144	
	$\rho$ alone	*	*	0.094	0.036	*	*	0.097	
	$\pi + \rho$	0.044	0.083	0.370	0.065	0.028	0.032	0.450	$0.41 \pm 0.13$
	$\pi - \rho$	0.044	0.083	0.095	0.018	0.028	0.032	0.033	
${}^4\text{He}$	$\pi$ alone	0.055	0.091	0.072	0.028	0.013	0.028	0.126	
	$\rho$ alone	*	*	0.074	0.032	*	*	0.077	
	$\pi + \rho$	0.055	0.091	0.293	0.050	0.013	0.028	0.369	$0.14 \pm 0.03$
	$\pi - \rho$	0.055	0.091	0.011	0.013	0.013	0.028	0.038	
${}^3\text{H}$	$\pi$ alone	0.044	0.072	0	0	0	0.056	0.013	
	$\rho$ alone	*	*	0	0	*	*	0	
	$\pi \pm \rho$	0.044	0.072	0	0	0	0.056	0.013	$0.29 \pm 0.14$

which leads to very small  $\Gamma_{nm}$  of  ${}^3\text{H}$  relative to those of  ${}^4\text{He}$  and  ${}^5\text{He}$ . This feature appears to be contradictory to the experimental one, though the data are not so accurate. We have considered  $\pi$  and  $\rho$ , but there seems to be no reason to leave out, for example,  $K$  and  $K^*$ . The assumption of  $SU_3$  symmetry on the weak and strong vertices of  $\pi$  and  $K$  leads to a similar strength of the decay interaction, but because of the heavier mass, the  $K$  contribution turns out by a couple of factors smaller than the  $\pi$  contribution. Concerning  $K^*$  compared with  $\rho$ , it would be natural to expect the same order of contribution. However, in view of the possible error involved in the  $\rho$  contribution, which could be by a factor of 3 or so,<sup>9)</sup> it would not be of much significance to talk about the  $K^*$  contribution independently. What has been learned in this note, in spite of such a large uncertainty, is that it seems to be difficult, within one boson exchanges, to suppress the tensor dominating character and simultaneously enhance the  ${}^3S_1 \rightarrow {}^3P_1$  decay channel. Thus the  $nm$  decay still remains to be one of the puzzling

problems in hypernuclear physics.

The authors would like to thank Professor Y. Shono and Professor K. Hasegawa for encouraging discussions.

- 1) M. M. Block and R. H. Dalitz, Phys. Rev. Lett. **11** (1963), 96.
- 2) W. Cheston and H. Primakoff, Phys. Rev. **92** (1953), 1537.
- 3) M. Ruderman and R. Karplus, Phys. Rev. **102** (1956), 247.
- 4) T. Tamiya, H. Kawaguchi and Y. Sumi, Prog. Theor. Phys. **34** (1965), 833.
- 5) T. Kohmura, Prog. Theor. Phys. **35** (1966), 65.
- 6) C. Itoh, Prog. Theor. Phys. **36** (1966), 761.
- 7) N. Panchapakesen, Phys. Lett. **20** (1966), 435.
- 8) J. B. Adams, Phys. Rev. **156** (1967), 1611.
- 9) B. H. J. McKellar and B. F. Gibson, Phys. Rev. **C30** (1984), 322.
- 10) C. Y. Cheng, D. P. Heddle and L. S. Kisslinger, Phys. Rev. **C27** (1983), 335.
- 11) Y. Yamamoto and H. Bandō, Prog. Theor. Phys.
- 12) M. M. Nagels, T. A. Rijken and J. J. deSwart, Phys. Rev. **D12** (1975), 744; **D15** (1977), 2547.